INJUN 5 OBSERVATIONS OF MAGNETOSPHERIC ELECTRIC FIELDS AND PLASMA CONVECTION

DONALD A. GURNETT

Dept. of Physics and Astronomy, The University of Iowa, Iowa City, Iowa, U.S.A.

Abstract. Recent measurements of magnetospheric electric fields with the satellite INJUN 5 have provided a comprehensive global survey of plasma convection at low altitudes in the magnetosphere. A persistent feature of these electric field observations is the occurrence of an abrupt reversal in the convection electric field at auroral zone latitudes. The plasma convection velocities associated with these reversals are generally directed E-W, away from the sun on the poleward side of the reversal, and toward the sun on the equatorward side of the reversal. Convection velocities over the polar cap region are normally less than those observed near the reversal region. The electric field reversal is observed to be coincident with the 'trapping boundary' for electrons with energies $E > 45$ keV. Near local noon the region of anti-sunward convection poleward of the electric field reversal/trapping boundary corresponds to the low altitude extension of the polar cusp plasma. Intense 'inverted V' electron precipitation events associated with auroral arcs are also observed near and poleward of the electric field reversal/trapping boundary. These observations are discussed in terms of a current model of magnetospheric convection.

1. Introduction

Recent measurements of electric fields using the double-probe technique on the low altitude (677 to 2528 km) polar orbiting satellite INJUN 5 have provided the first extensive global survey of electric fields and plasma convection in the magnetosphere. In this paper we summarize the principal observational results from the electric field experiment on this spacecraft.

The electric field experiment on INJUN 5 is of the double-probe type described by Fahleson (1967) and others. The probes used consist of two conducting spheres 20.3 cm in diameter mounted on booms with a center-to-center separation of 2.85 m. The spacecraft is magnetically oriented by a bar magnet within the spacecraft such that the electric antenna axis is maintained approximately perpendicular ($\sim \pm 10°$) to the geomagnetic field. The potential difference between the spheres is obtained from a high input impedance differential amplifier and is recorded, along with other data, by a tape recorder in the satellite so that global surveys of electric fields and other geophysical phenomena can be obtained. Various other parameters such as the antenna impedance and the electron density and temperature are also available to determine if the electric antenna system is operating properly. For further details on the INJUN 5 electric field instrumentation and observations the reader is referred to papers by Gurnett *et al.* (1969), Gurnett (1970), Cauffman and Gurnett (1971, 1972), and Frank and Gurnett (1971).

2. Data Analysis and Instrumental Effects

Electric field measurements obtained for a pass over the northern polar region are shown in Figure 1 to illustrate the technique used in analyzing the INJUN 5 electric

B. M. McCormac (ed.), Earth's Magnetospheric Processes, 233–245.

field data. The systematic sinusoidal variation evident in the measured electric field E_m (shown by the light line in the top panel of Figure 1) is caused by the spacecraft rotation in the $\mathbf{V}_s \times \mathbf{B}$ field from the spacecraft motion through the ionosphere. At middle and low latitudes, where the ionospheric plasma is expected to corotate with the earth, the $\mathbf{V}_s \times \mathbf{B}$ field provides a convenient reference for 'calibrating' the overall accuracy of the electric field determination. After all instumental effects are considered

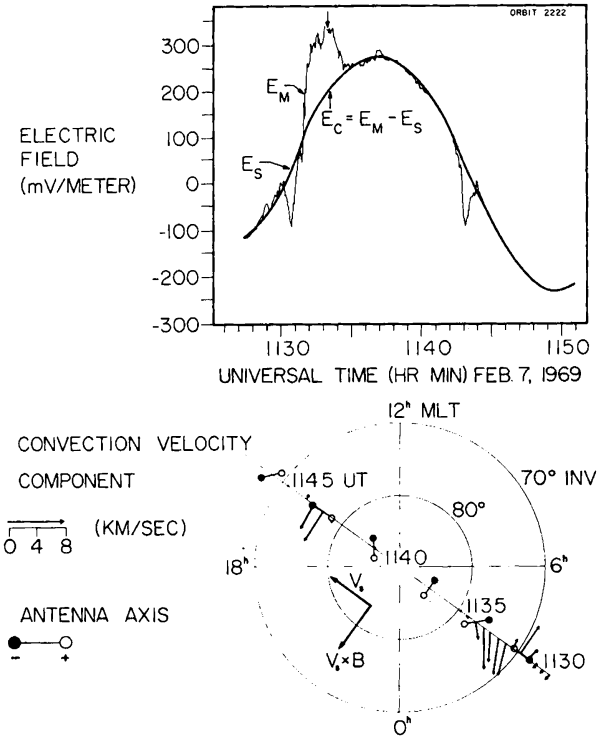

Fig. 1. Method of subtracting the $\mathbf{V}_S \times \mathbf{B}$ electric field, E_S, from the measured electric field, E_m, to determine the convection electric field, $E_c = E_m - E_S$, and a polar plot of the associated convection velocity component.

the overall accuracy of the INJUN 5 electric field measurements, as determined by comparisons with the $\mathbf{V}_s \times \mathbf{B}$ field, is about ± 30 mV m^{-1}. This error is primarily caused by unequal photoelectron emission from the two spheres due to asymmetrical sunlight shadowing of the spheres by the supporting booms. For certain orientations and for cases when the spacecraft is rotating very slowly, the effects of this asymmetrical shadowing can be eliminated and the accuracy is increased to about ± 10 mV m^{-1}.

To determine naturally occurring convection electric fields it is necessary to subtract the $\mathbf{V}_s \times \mathbf{B}$ field and errors due to shadowing asymmetries from the measured

electric field. The procedure used to determine the subtracted electric field, E_s, is to (a) compute the expected $\mathbf{V}_s \times \mathbf{B}$ field component using the estimated spacecraft orientation (which is sometimes in error by up to 10° in rotation about the geomagnetic field), and then to (b) readjust the amplitude and phase of the sinusoidal $\mathbf{V}_s \times \mathbf{B}$ variations to provide a good fit to the observed $\mathbf{V}_s \times \mathbf{B}$ field at low latitudes where no convection electric fields are expected. The solid dark curve shown in the top panel of Figure 1 is the subtracted electric field, E_s, determined in this manner. The difference between the measured electric field and the subtracted electric field, $E_c = E_m - E_s$, is the best estimate of the actual convection electric field in the ionosphere. Other readily recognizable errors due to sunlight shadowing by the spacecraft body and wake effects must also be eliminated from consideration (see Cauffman and Gurnett (1971) for a discussion of these effects).

The plasma convection velocity $\mathbf{V}_c$ is determined from the convection electric field $\mathbf{E}_c$ using the equation (Axford, 1969)

$$\mathbf{V}_c = \mathbf{E}_c \times \mathbf{B}/B^2 .$$

The convection velocity components corresponding to the electric field measurements in the top panel of Figure 1 are shown by the arrows in the IN Lat-MLT polar diagram at the bottom of Figure 1. The direction of the arrow represents the direction of the convection velocity component detected and the length of the arrow is proportional to the magnitude of the convection velocity. Note that the arrows do *not* indicate the vector direction of the convection velocity since only one component is measured.

3. Summary of Observations

The convection observations shown in Figures 2 and 3 have been selected to illustrate some of the general features of the INJUN 5 convection electric field measurements. The most prominent and persistent feature of the INJUN 5 electric field data is the occurrence of an abrupt reversal or discontinuity in the convection electric field at about 70 to 80° IN Lat. An example of such an electric field reversal is shown in Figure 1 at 1132 UT where the convection electric field changes sign, from about -100 to $+125$ mV m^{-1}. The corresponding convection velocity component (shown in the polar diagram at the bottom of Figure 1) shows a reversal from eastward (sunward) flow on the equatorward side of the reversal to westward (anti-sunward) flow on the poleward side of the reversal. The series of successive dawn-dusk polar passes illustrated in Figure 2 also show similar abrupt reversals in the direction of the convection velocity. These reversals are particularly evident in the dawn LT region at about 1724:20, 1925:30, and 2123:30 UT. Smaller reversals are also evident in the dusk region at 1734:00 and 2132:00 UT. In all cases the reversals are consistent with a generally sunward flow on the equatorward side of the reversal and anti-sunward flow on the poleward side of the reversal.

Usually the largest convection velocities are observed near (within 5 to 10° IN Lat) the electric field reversal location. At higher latitudes, in the polar cap region, the

convection velocity is usually less than the ~ 0.75 km s^{-1} sensitivity limit imposed by the ± 30 mV m^{-1} uncertainty in the convection electric field determination. Orbit 6909 (Figure 2), however, shows the occurrence of an essentially uniform antisunward flow with velocities greater than 1 km s^{-1} along the entire satellite trajectory

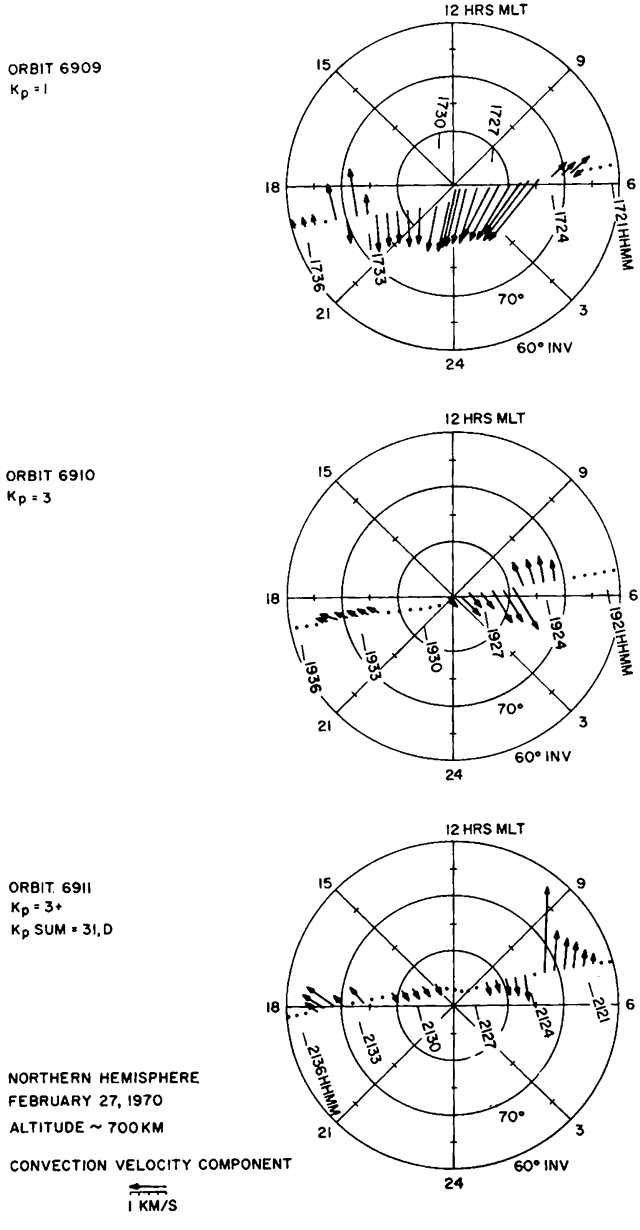

Fig. 2. A series of dawn-dusk orbits showing the persistent occurrence of reversals in the convection electric field in both the dawn and dusk regions, and one case (orbit 6909) having nearly constant antisunward convection along the entire satellite trajectory over the polar cap region.

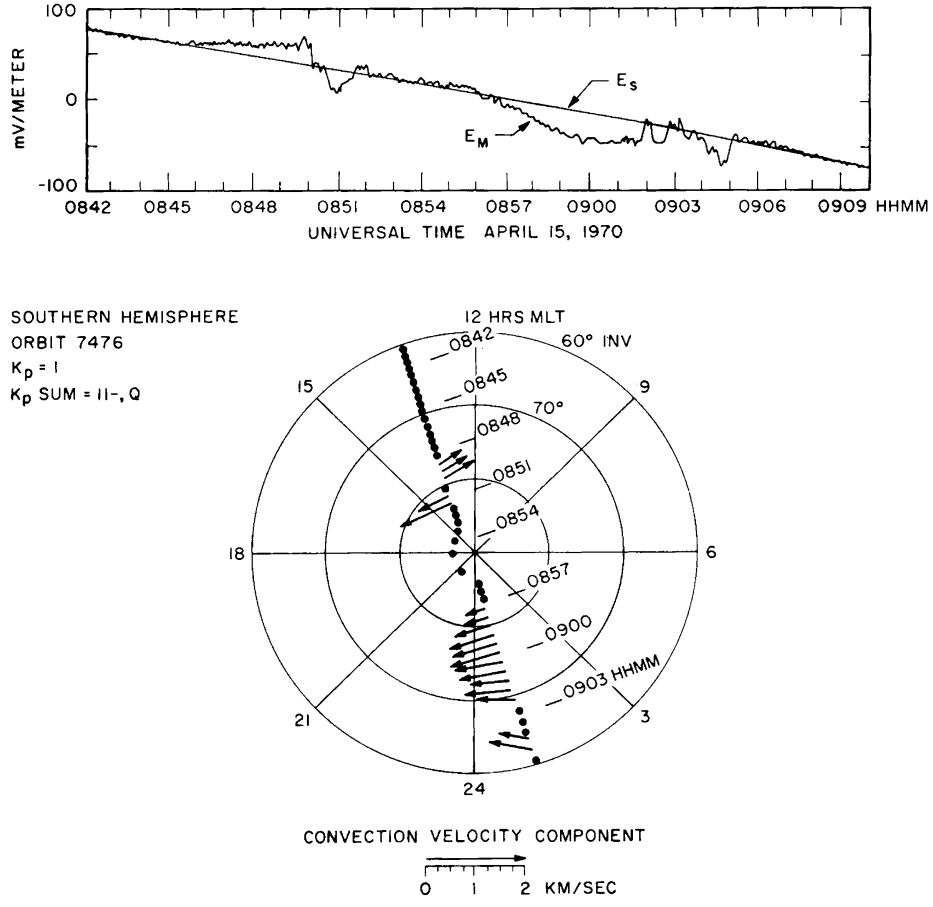

Fig. 3. A noon-midnight pass showing a distinct reversal near local noon at about 80° IN Lat, relatively low convection velocities over the polar cap, and a large zone of westward convection in the local midnight region.

over the polar region from 1724:00 to 1734:00 UT. Examples of relatively uniform transpolar convection, such as might be inferred from cases like orbit 6909, with convection velocities greater than 0.75 km s^{-1} are not commonly observed with INJUN 5.

Figure 3 illustrates the electric field observed for an approximately noon-midnight meridonal pass over the southern hemisphere. Near local noon, at about 0850:20 UT and 80° IN Lat, a clearly defined electric field reversal is observed. Over the polar cap region, from about 0852:00 to 0857:00, the convection velocity component detected is very small, less than 0.25 km s^{-1}. The spacecraft orientation and rotation rate for this pass is such that the convection velocity can be determined to within about 0.25 km s^{-1} (± 10 mV m^{-1}). In the local midnight region a large westward (anti-sunward) convection zone is observed from 0857:00 to 0902:00 UT and a variety of more complex variations is observed after 0902:00 UT. In this case, no

discernible electric field reversal is observed in the local midnight region. The INJUN 5 electric field observations through the noon-midnight LT regions generally tend to be more complex and less ordered than in the dawn-dusk regions, particularly near local midnight, with a tendency for multiple zones of convection and more than one electric field reversal or, as in the case shown, no electric field reversal at all.

In order to obtain a general idea of the average or 'typical' high latitude convection pattern a study was performed (Cauffman and Gurnett, 1972) using all of the available INJUN 5 electric field data. Since only one component of the electric field is sensed it is necessary to utilize a large number of observations at different antenna orientations to deduce the general direction of the plasma flow. The method used to determine the general direction of the plasma flow was to analyze all of the observed electric field reversals in terms of either E-W or N-S velocity components on either side of the reversal. Figure 4 shows the results of interpreting all of the observed reversals in terms of E-W convection. Each point represents the position of an electric field reversal. The open circles indicate that the convection velocity is eastward on the poleward side of the reversal and westward on the equatorward side of the reversal.

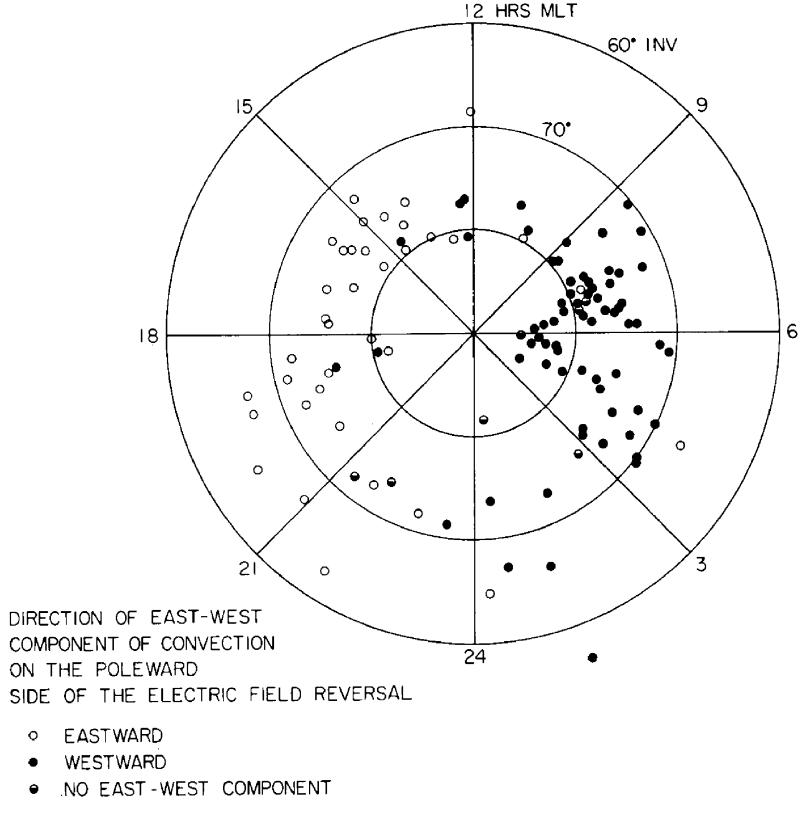

Fig. 4. Locations of reversals observed by INJUN 5, coded to indicate the E-W direction of the convection poleward and equatorward of the reversal.

The dark circles indicate the opposite, westward on the poleward side and eastward on the equatorward side. The half dark circles represent cases where the electric antenna orientation was such that only the N-S component of the convection velocity could be sensed.

From Figure 4 it is seen that for LT's from 0 to 12 hr the convection velocity is generally westward (antisunward) on the poleward side of the reversal and eastward (sunward) on the equatorward side of the reversal. For LT's from 12 to 24 hr the latitudinal variation is just the opposite. A similar scatter plot obtained by analyzing all of the reversals in terms of N-S convection components shows no consistent ordering of the data, thereby indicating that the convection velocities at the reversal boundary are primarily E-W.

The general convection pattern deduced from the INJUN 5 observations is illustrated schematically in Figure 5. This diagram incorporates the results from the statistical study discussed above indicating that near the reversal the plasma flow is

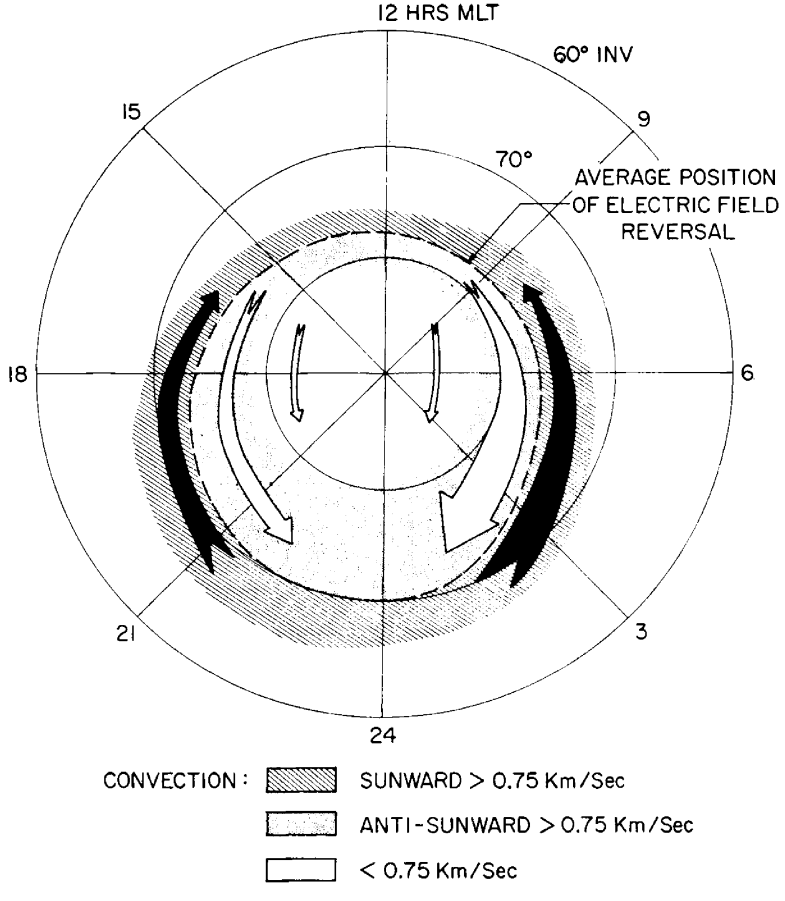

Fig. 5. Qualitative sketch summarizing the 'average' convection pattern obtained from the INJUN 5 electric field measurements.

primarily E-W, away from the sun on the poleward side of the reversal, and toward the sun on the equatorward side of the reversal. The large arrows near the reversal boundary are indicative of the fact that the largest convection velocities are usually observed within about 5 to 10° IN Lat from the reversal boundary. The larger arrows in the dawn region compared to the dusk region are indicative of the fact that the convection velocities are usually largest in the dawn LT region (cf., Figure 2). The narrowing of the arrows toward local noon is indicative of the fact that the latitudinal width of the convection zones tends to be narrower near local noon and wider in the local evening (cf., Figure 3). The smaller arrows over the polar cap region reflect the fact that the convection velocities are generally smaller (<0.75 km s^{-1}) over the polar cap region than near the reversal boundary. The anti-sunward direction of the convection in the polar cap region is based on the recent electric field measurements by Maynard (1971) with the OGO 6 satellite which reportedly show a general anti-sunward flow over the polar cap region with velocities generally below the 0.75 km s^{-1} sensitivity limit of the INJUN 5 electric field experiment.

It should be emphasized that the convection pattern illustrated in Figure 5 represents a gross average of the convection detected by INJUN 5 and significant departures undoubtedly occur. Since, in many cases, the convection velocity is below the sensitivity limit of the INJUN 5 electric field experiment, the convection pattern in Figure 5 represents conditions of enhanced convection (>0.75 km s^{-1}) and may not be representative of more quiescent conditions.

4. Association with Charged Particle Observations

Comparisons of the low energy charged particle measurements from the LEPEDEA instrumentation on INJUN 5 and the electric field data have shown that the electric field reversal corresponds closely with the position of the 'trapping boundary' for electrons with energies $E>45$ keV (Frank and Gurnett, 1971). (See Frank and Ackerson (1971) for details of the LEPEDEA instrumentation.) An example of this association is illustrated in Figure 6 which shows the electric field and selected charged particle measurements for a dawn-dusk pass over the northern polar region. Because of the favorable antenna orientation and very slow rotation rate on this pass the convection electric field can be determined to an accuracy of about ± 10 mV m^{-1}. A clearly defined electric field reversal is observed at about 1443:20 UT in the dawn LT region and a smaller, less distinct, reversal is observed at about 1453:10 UT in the dusk LT region. These electric field reversals are seen to be essentially coincident with the high latitude termination of measurable intensities of electrons with energies $E>45$ keV (indicated by the dashed vertical lines in Figure 6). This termination is commonly referred to as the 'trapping boundary' and represents a natural coordinate for investigating high latitude magnetospheric phenomena (Frank and Ackerson, 1972). On the basis of these and other measurements, Frank and Gurnett (1971) have interpreted the trapping boundary and associated electric field reversal as delineating the high latitude termination of closed field lines, with the sunward

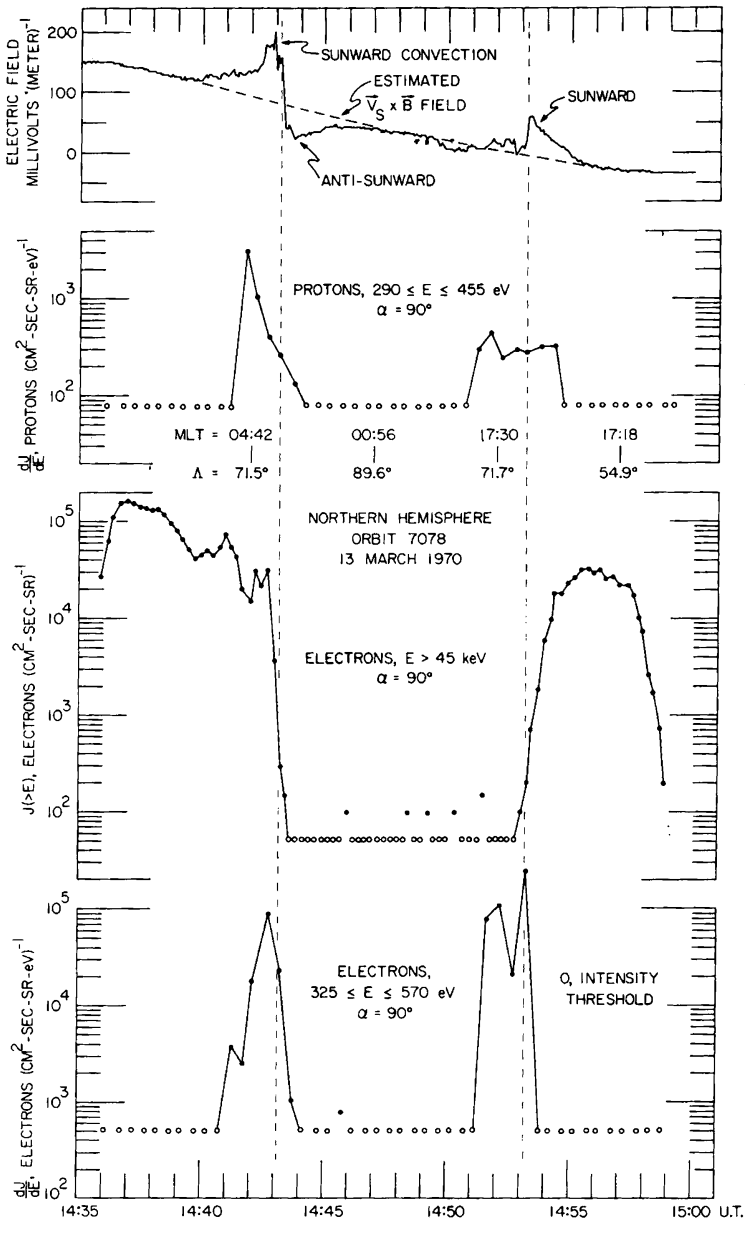

Fig. 6. Simultaneous electric fields and low energy plasma measurements showing the correspondence between the electric field reversal, the $E > 45$ keV trapping boundary, and inverted 'V' electron precipitation events.

plasma flow occurring on closed field lines within the magnetosphere, and the anti-sunward plasma flow occurring on open field lines which connect into the solar wind.

Low energy electron precipitation events associated with auroral arcs are also observed near and sometimes poleward of the trapping boundary/electric field

reversal location. These low energy electron precipitation events often have a characteristic 'inverted V' energy-time signature with the average electron energy increasing from less than 100 eV to a maximum of several keV, or more, subsequently decreasing as the satellite passes through the precipitation region (Frank and Ackerson, 1971a). Inverted 'V' precipitation events have been directly associated with auroral arcs (Ackerson and Frank, 1971). The low energy ($325 \leqslant E \leqslant 570$ eV) electron fluxes shown in the bottom panel of Figure 6 provide a coarse indication of the location of inverted 'V' electron precipitation events occurring during this pass. In the local morning region a single inverted 'V' event is observed at approximately 1443 UT, nearly coincident with the trapping boundary/electric field reversal location. In the local evening region two inverted 'V' events are observed, one at about 1453 UT, near the trapping boundary, and the second at about 1452 UT, poleward of the trapping boundary.

The relative locations of the inverted 'V' events and the trapping boundary in this case are consistent with the general survey results of Frank and Ackerson (1972) which show that the inverted 'V' precipitation events occur on open field lines near or poleward of the $E > 45$ trapping boundary and in a region of generally anti-sunward convection (cf., Figure 5). Equatorward of the $E > 45$ keV trapping boundary, in the region of sunward convection, significant electron precipitation and associated auroral light emission are also observed during the local midnight and morning hours. However, the electron precipitation in this region generally has a harder energy spectrum and lower intensity than the inverted 'V' events and is identified by Frank and Ackerson (1971) as originating from plasma sheet electrons injected onto closed field lines in the local midnight region.

Near local noon the convection electric fields observed by INJUN 5 can be directly associated with the entry of magnetosheath plasma into the polar magnetosphere through the dayside polar cusp region identified by Frank (1971a), Frank and Ackerson (1971), and Heikkila and Winningham (1971). An example of such an observation is shown in Figure 7, from Gurnett and Frank (1972). The intense fluxes of low energy electrons ($325 \leqslant E \leqslant 570$ eV) and protons ($290 \leqslant E \leqslant 455$ eV) occurring from 1511:30 to 1513:45 UT on this pass, poleward of the $E > 45$ keV trapping boundary, identify this region as the polar cusp. The separation of the polar cusp into an equato-r ward 'electron sheet' and a poleward 'proton sheet' is directly comparable to Frank's (1971a) IMP 5 observations of the polar cusp at much higher altitudes, $\sim 5\ R_E$. The simultaneous observation of broadband VLF hiss generated by the polar cusp plasma (shown in the top panel of Figure 7) provides further evidence of the polar cusp location on this pass. The electric field data for this pass show a negative perturbation from the $\mathbf{V}_s \times \mathbf{B}$ field of about 30 mV m^{-1} in the polar cusp region. This electric field corresponds to a westward (anti-sunward) convection of about 1 km s^{-1} in the polar cusp region. From this and other similar observations it is concluded that the polar cusp region is directly associated with the region of enhanced anti-sunward convection on the poleward side of the electric field reversal/trapping boundary (cf., Figure 5).

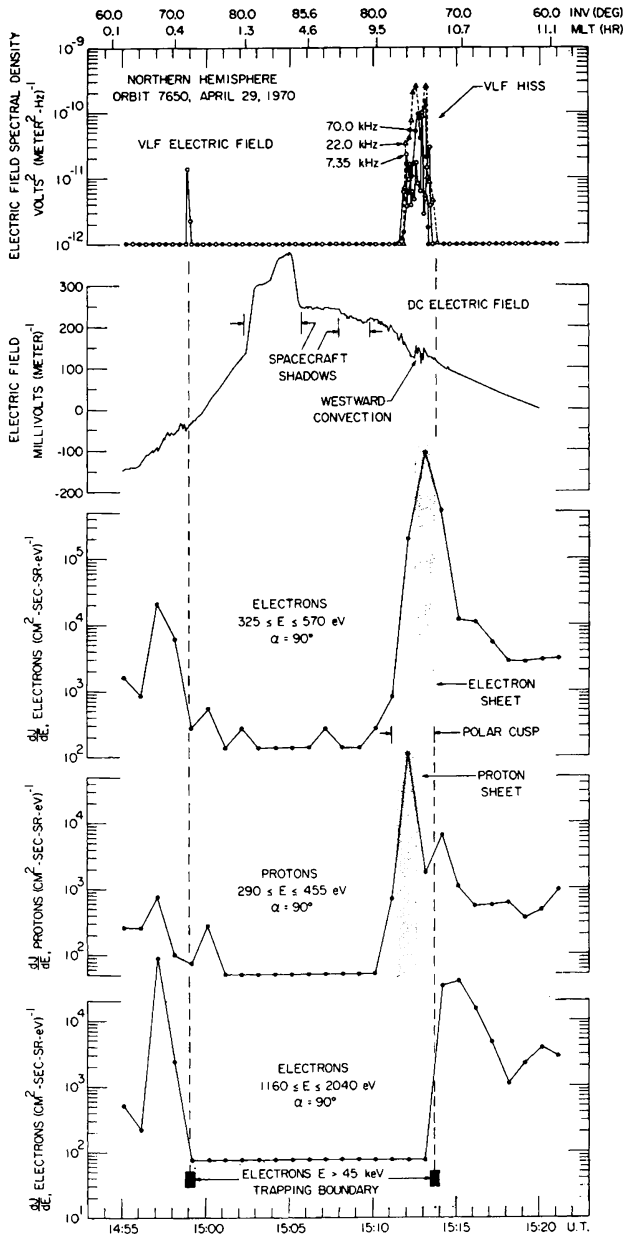

Fig. 7. Simultaneous VLF, electric field, and low energy plasma observations showing the occurrence of anti-sunward (westward in this case) convection in the polar cusp region.

5. Discussion

The general pattern of low altitude convection can be interpreted using the magnetospheric model shown in Figure 8 (Frank and Gurnett, 1971). This model uses the

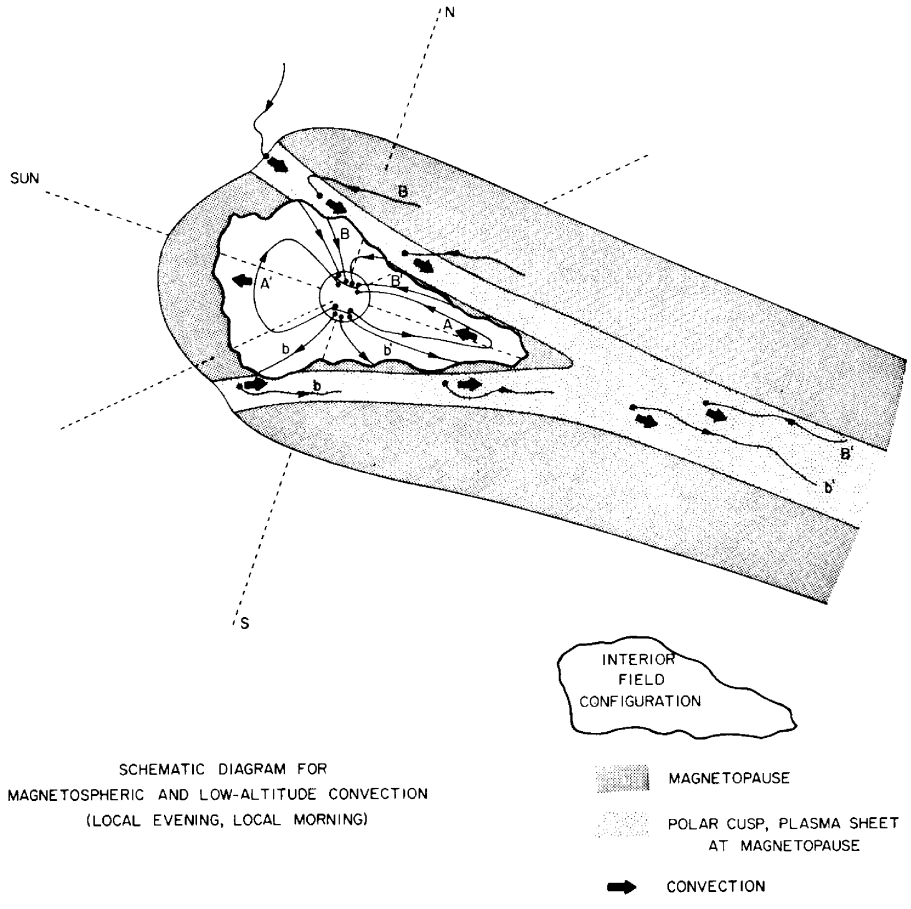

Fig. 8. Schematic diagram showing the proposed model of magnetospheric convection. The electric field reversal and the $E > 45$ keV trapping boundary occur at the boundary between open (B–b and B′–b′) and closed (A and A′) field lines.

process of merging the geomagnetic field with the solar wind magnetic field proposed by Dungey (1961, 1968), along with the usual 'frozen field' model of plasma flow to explain the coupling of the solar wind convection into a magnetosphere; however, it differs from Dungey's model in the details of the flow over the polar cap region. Magnetic merging along the sunward surface of the magnetosphere allows the direct connection of geomagnetic field lines with the solar wind magnetic field. On the dayside of the magnetosphere, these field lines constitute open field lines through the polar cusp (such as B and b in Figure 8) and provide for the direct entry of magnetosheath plasma to low altitudes within the magnetosphere. Since the plasma convection away from the sun on the dayside of the magnetosphere is usually limited to a relatively narrow zone on the poleward side of the trapping boundary (cf., Figures 3 and 7) the convective flow in the polar cusp region is believed to follow the E-W extension of the polar cusp into the dawn and dusk flanks of the magnetosphere as indicated in

Figure 8. The width of this convection zone, which is initially only a few degrees wide in IN Lat near local noon, increases considerably in the dawn and dusk regions. Subsequent anti-sunward convection carries the field lines into the distant plasma sheet (field lines B′ and b′) where they again merge to form closed field lines (such as A) in the near earth plasma sheet. (The reader is referred to Frank (1917b) for a discussion of the various plasma regimes involved in this model.) After merging occurs at the neutral sheet the field lines are then convected sunward, toward the front of the magnetosphere (field line A′) to complete the flow pattern. This flow pattern for magnetospheric plasma qualitatively accounts for the principal features of the observed convection pattern at low altitudes (cf., Figure 5). It is to be noted that in this model the electric field reversal, which is the boundary between the regions of sunward and anti-sunward flow, occurs on field lines which are in the merging region. Since magnetic merging constitutes a basic process by which energy is dissipated within the magnetosphere, it is understandable that intense electron acceleration and precipitation are associated with the electric field reversals, although the details of these processes remain to be resolved.

Acknowledgments

This research was supported in part by the National Aeronautics and Space Administration under contracts NAS5-10625, NAS1-8141, NAS1-8144(f), NAS1-8150(f), and NGL-16-001-043; and by the Office of Naval Research under Contract N00014-68-A-0196-0003.

References

Ackerson, K. L. and Frank, L. A.: 1971, *J. Geophys. Res.* to be published.
Axford, W. I.: 1969, *Rev. Geophys.* **7**, 421.
Cauffman, D. P. and Gurnett, D. A.: 1971, *J. Geophys. Res.* **76**, 6014.
Cauffman, D. P. and Gurnett, D. A.: 1972, *Space Sci. Rev.*, submitted.
Dungey, J. W.: 1961, *Phys. Rev. Letters*, **6**, 47.
Dungey, J. W.: 1968, in B. M. McCormac (ed.), *Earth's Particles and Fields*, Reinhold Book Corporation, New York, p. 385.
Fahleson, U. V.: 1967, *Space Sci. Rev.* **7**, 238.
Frank, L. A.: 1971a, *J. Geophys. Res.* **76**, 5202.
Frank, L. A.: 1971b, *J. Geophys. Res.* **76**, 2512.
Frank, L. A. and Ackerson, K. L.: 1971, *J. Geophys. Res.* **76**, 3612.
Frank, L. A. and Ackerson, K. L.: 1972, *J. Geophys. Res.*, submitted.
Frank, L. A. and Gurnett, D. A.: 1971, *J. Geophys. Res.* **76**, 6829.
Gurnett, D. A.: 1970, in B. M. McCormac (ed.), *Particles and Fields in the Magnetosphere*, D. Reidel Publishing Company, Dordrecht, Holland, p. 239.
Gurnett, D. A. and Frank, L. A.: 1972, *J. Geophys. Res.* **77**, 172.
Gurnett, D. A., Pfeiffer, G. W., Anderson, R. R., Mosier, S. R., and Cauffman, D. P.: 1969, *J. Geophys. Res.* **74**, 4631.
Heikkila, W. J. and Winningham, J. D.: 1971, *J. Geophys. Res.* **76**, 883.
Maynard, N. C.: 1971, *Electric Fields in the Ionosphere and Magnetosphere*, presented at the Advanced Study Institute on Magnetosphere-Ionosphere Interactions, Dalseter, Norway, April 14–23.